Chinese Chemical Letters 35 (2024) 108539

Contents lists available at ScienceDirect

Chinese Chemical Letters

journal homepage: www.elsevier.com/locate/cclet

Mitochondria-targeted Janus mesoporous nanoplatform for tumor photodynamic therapy

Min Dong[a,1], Rui Tang[a,1], Jing Li[a], Jiajia Zhao[a], Yu Wang[a], Lin Ouyang[c,*], Wei Lu[a], Jun Tao[a], Meng Dang[d], Yuxia Tang[b,*], Zhaogang Teng[a,*]

[a] Key Laboratory for Organic Electronics & Information Displays and Jiangsu Key Laboratory for Biosensors, Institute of Advanced Materials, Jiangsu National Synergetic Innovation Centre for Advanced Materials, Nanjing University of Post and Telecommunications, Nanjing 210023, China
[b] Laboratory of Molecular Imaging, Department of Radiology, The First Affiliated Hospital of Nanjing Medical University, Nanjing 210029, China
[c] Department of Radiology, The 909th Hospital, Southeast Hospital, School of Medicine, Xiamen University, Zhangzhou 363000, China
[d] State Key Laboratory for Modification of Chemical Fibers and Polymer Materials, College of Materials Science and Engineering, Institute of Functional Materials, Donghua University, Shanghai 201620, China

ARTICLE INFO

Article history:
Received 2 November 2022
Revised 25 March 2023
Accepted 5 May 2023
Available online 8 May 2023

Keywords:
Mesoporous materials
Janus particle
Photodynamic therapy
Mitochondria targeting
Tumor treatment

ABSTRACT

Photodynamic therapy (PDT) is an effective treatment method for tumors. But the specifically accumulated of photosensitizer was very difficult in the tumor site, which greatly limited the efficacy of PDT. Here, mitochondria-targeted Janus mesoporous nanoplatform (JPMO-Pt-CTPP-ZnPc) for PDT was prepared, the nanoplatform has uniform size (275 nm) and good dispersion and biocompatibility. The confocal laser scanning microscopy (CLSM) revealed the signal of ZnPc of JPMO-Pt-CTPP-ZnPc were higher than JPMO-Pt-ZnPc in tumor cells, and flow cytometry results showed the cell uptake efficiency of JPMO-Pt-CTPP-ZnPc was 2.5-fold higher than that of JPMO-Pt-ZnPc. This revealed the modification of CTPP significantly improves the targeting ability of the nanoplatform. *In vitro* anti-tumor experiment showed the JPMO-Pt-CTPP-ZnPc significantly inhibited the growth of tumor cells upon the irradiation of low-power laser, and the survival rate of cells incubated with 60 μg/mL JPMO-Pt-CTPP-ZnPc was only 3%. Simultaneously, compared with JPMO-Pt-ZnPc (not modified with mitochondria targeting molecules CTPP), the PDT efficacy of JPMO-Pt-CTPP-ZnPc was significantly better, as it has targeted mitochondria in cells.

Photodynamic therapy (PDT) is an effective treatment method for tumors [1–13]. PDT stimulates the photosensitizer to produce reactive oxygen species (ROS) upon exposure to light, thereby inducing tumor cell damage [14–17]. PDT mainly relies on photosensitizers, light with specific wavelengths, and oxygen [18,19]. It is not invasive, shows no obvious drug resistance, and results in few side effects. However, there are still problems with PDT that must be overcome [20–22]. First, photosensitizers are mostly aromatic or porphyrin molecules with poor solubility in water and a tendency to aggregate [23], which results in biological toxicity and limits the effective dose of photosensitizers. Second, photosensitizers are degraded in blood circulation, resulting in a low utilization rate. Most importantly, photosensitizers do not specifically accumulate at the tumor site [24,25], which substantially limits the effect of PDT [26]. As approaches to solve these problems, researchers have synthesized many nanoplatforms for PDT to improve the water solubility of photosensitizers and to enable them to specifically act on tumor tissues [27].

Mitochondria are the power stations of cells and regulate many biological processes in cells, including biosynthesis, signal transduction, and apoptosis [28]. Based on accumulating evidence, mitochondria play a vital role in tumor biological processes (tumor development, growth, metastasis, *etc.*), which all require mitochondria to provide energy support [29]. Recently, the use of mitochondria as tumor treatment targets has attracted extensive attention from researchers [30–34]. Notably, the increase in the mitochondrial ROS content may activate the cell death mechanism. Therefore, PDT targeting mitochondria is an effective treatment method for tumors [35]. However, the development of a more efficient strategy to increase the mitochondrial ROS content in tumor cells remains a challenge.

In this study, we used a Janus nanoplatform consisting of periodic mesoporous organosilica-coated platinum nanoplatforms (JPMO-Pt) as the carrier of zinc phthalocyanine (ZnPc, a photosensitizer) and modified the JPMO-Pt surface with (3-carboxy-

* Corresponding authors.
E-mail addresses: ddcqzg@126.com (L. Ouyang), tangyuxia5@163.com (Y. Tang), iamzgteng@njupt.edu.cn (Z. Teng).
[1] These authors contributed equally to this work.

https://doi.org/10.1016/j.cclet.2023.108539
1001-8417/

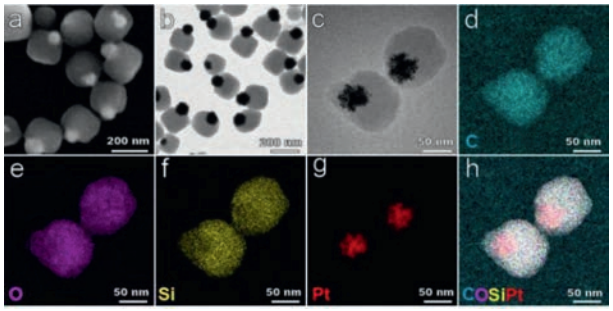

Fig. 1. (a) SEM and (b, c) TEM images of the JPMO-Pt at different magnifications. (d–g) EDX elemental mapping of C, O, Si and Pt elements and (h) the merged elemental images.

propyl)triphenylphosphonium bromide (CTPP, a mitochondria-targeting molecule) to construct a photodynamic nanoplatform targeting mitochondria. The prepared JPMO-Pt-CTPP-ZnPc had uniform size, good dispersity, and biocompatibility. The JPMO-Pt-CTPP-ZnPc effectively targeted the mitochondria of tumor cells to achieve efficient PDT for tumors. The results of cell-based experiments indicated that compared with JPMO-Pt-ZnPc, JPMO-Pt-CTPP-ZnPc had a stronger mitochondria-targeting effect and a greater killing effect on tumor cells.

We used the amphiphilic block polymer F127 as the structure-directing agent and H_2PtCl_6 as the precursor to synthesize mesoporous Pt nanoparticles. TEM and SEM images (Fig. S1 in Supporting information) revealed that the synthesized Pt had a good dispersity and uniform size (diameter: approximately 95 nm). Then, mesoporous organosilica was deposited on one side of the mesoporous Pt nanoparticles using 1,2-bis(triethoxysilyl)ethane as the precursor and cetyltrimethylammonium bromide as the surfactant to prepare the JPMO-Pt [36,37]. SEM and TEM images (Figs. 1a–c) revealed that the synthesized JPMO-Pt had a good dispersity and uniform size (diameter: approximately 244 nm). The elemental maps of C, O, Si and Pt in the JPMO-Pt (Figs. 1d–h) demonstrated that Pt only existed on the fringes of the nanocomposite structure, while most O, C and Si atoms were evenly distributed in the mesoporous organosilica on the periphery of Pt. The results further suggested that the JPMO-Pt is a Janus structured nanocomposites [38–40].

The results of Fourier transform infrared spectroscopy indicated the JPMO-Pt-CTPP had two more absorption peaks than the JPMO-Pt in the interval of 1400–1600 cm^{-1} (Fig. 2a). These two absorption peaks were derived from the characteristic peaks of the benzene ring skeleton of the CTPP, indicating that the JPMO-Pt was successfully modified with CTPP. We used JPMO-Pt-CTPP to adsorb ZnPc (a photosensitizer) and enable JPMO-Pt to be used in PDT of tumors. The Fourier transform infrared spectroscopy of JPMO-Pt-CTPP-ZnPc had more absorption peaks than the JPMO-Pt-CTPP in the interval of 1400–1600 cm^{-1}, demonstrating the successfully loading of ZnPc (Fig. S2 in Supporting information). The drug loading content of ZnPc in the nanoplatform was approximately 13%. The UV–visible spectra (Fig. 2b) indicated that ZnPc had absorption peaks at 606 nm and 666 nm, and the absorption peak at 666 nm was a distinct strong absorption peak with the highest intensity. A comparison of the UV–vis spectra before and after loading ZnPc revealed that the JPMO-Pt-ZnPc and JPMO-Pt-CTPP-ZnPc exhibited significantly stronger absorption than the JPMO-Pt from 600 nm to 800 nm, which further confirmed that the JPMO-Pt-CTPP successfully adsorbed ZnPc. We stably modified the surface with CTPP (a mitochondria-targeting molecule) to enable JPMO-Pt to target mitochondria. First, the surface of JPMO-Pt was modified with amino groups. The dynamic light scattering results indicated that the diameters of the JPMO-Pt, JPMO-Pt-CTPP and JPMO-Pt-CTPP-ZnPc

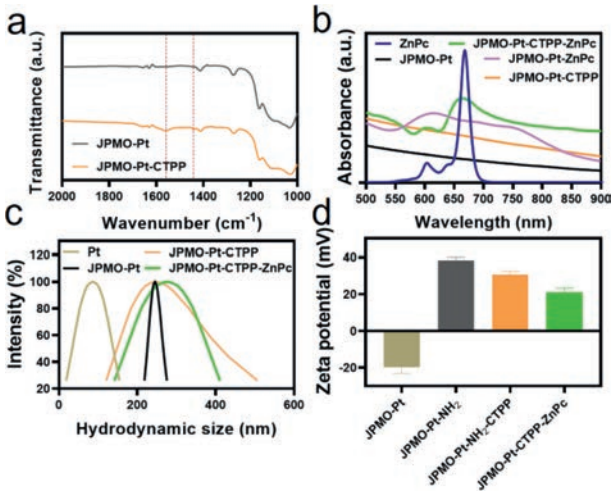

Fig. 2. (a) Fourier transform infrared spectra of JPMO-Pt and JPMO-Pt-CTPP. (b) UV–visible spectra of ZnPc, JPMO-Pt, JPMO-Pt-ZnPc, JPMO-Pt-CTPP and JPMO-Pt-CTPP-ZnPc. (c) Hydrodynamic sizes of Pt, JPMO-Pt, JPMO-Pt-CTPP, JPMO-Pt-CTPP-ZnPc. (d) Zeta potentials of JPMO-Pt, JPMO-Pt-NH_2, JPMO-Pt-NH_2-CTPP, and JPMO-Pt-CTPP-ZnPc.

were 245, 271 and 275 nm, respectively (Fig. 2c), respectively, indicating that the JPMO-Pt-CTPP-ZnPc had good dispersity and stability. The zeta potential (Fig. 2d) indicated that JPMO-Pt was electronegative with a potential of approximately −19.1 mV after the removal of the surfactant CTAB, and the JPMO-Pt became electropositive with a potential of +38.2 mV after amino modification. The change in the potential indicated that the surface of JPMO-Pt was successfully modified with amino groups. Next, we successfully obtained the nanocomposite particles with a mitochondria-targeting function (JPMO-Pt-CTPP) by linking the activated CTPP to the amino groups on the surface of JPMO-Pt through amidation. The zeta potential (Fig. 2d) demonstrated that the surface potential of the JPMO-Pt-CTPP was approximately +30.5 mV, which was approximately 7.7 mV lower than the surface potential of JPMO-Pt-NH_2 at the same concentration. This difference is because the reaction between CTPP and amino groups on the JPMO-Pt, further confirming the successful modification of the JPMO-Pt with CTPP.

Then mitochondrion targeting of JPMO-Pt-CTPP-ZnPc in 4T1 cells was evaluated by confocal laser scanning microscopy (CLSM) and the results were shown in Fig. 3a. The obvious co-localized fluorescent signals (yellow) from the ZnPc and mitochondria revealed that mitochondria-targeting efficiencies of JPMO-Pt-CTPP-ZnPc were higher than JPMO-Pt-ZnPc. That is, JPMO-Pt-CTPP-ZnPc exhibited targeted accumulation in mitochondria. Furthermore, we have investigated the 3D colocalization of JPMO-Pt-CTPP-ZnPc in 4T1 cells and the results showed that JPMO-Pt-CTPP-ZnPc localized in the mitochondrion compared to JPMO-Pt-ZnPc (Fig. S3 in Supporting information).

Next, the cellular uptake of JPMO-Pt-CTPP-ZnPc and JPMO-Pt-ZnPc in 4T1 cells was quantified using flow cytometry. As shown in Fig. 3b, the fluorescent intensity of ZnPc in 4T1 cells incubated with JPMO-Pt-CTPP-ZnPc was significantly higher than that of JPMO-Pt-ZnPc. The median fluorescent intensity of ZnPc in 4T1 cells incubated with JPMO-Pt-CTPP-ZnPc was approximatively 2.5-fold higher than that in 4T1 cells incubated with JPMO-Pt-ZnPc (Fig. 3c). These results demonstrate that the modification of CTPP significantly improves the mitochondrion-targeting ability and much higher 4T1 cancer cell accumulation.

Finally, we evaluated the cytocompatibility of the JPMO-Pt, JPMO-Pt-ZnPc, and JPMO-Pt-CTPP-ZnPc. MTT experiments indicated that after the cells were incubated with different concentrations of JPMO-Pt, JPMO-Pt-ZnPc, and JPMO-Pt-CTPP-ZnPc for 24

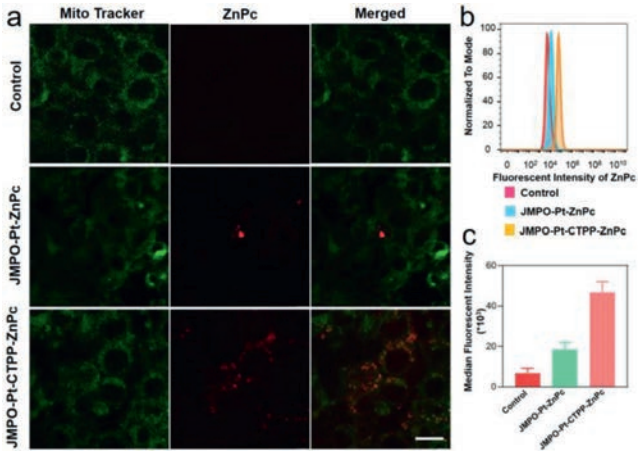

Fig. 3. (a) Imaging of mitochondrial colocalization in 4T1 cells incubated with JPMO-Pt-ZnPc or JPMO-Pt-CTPP-ZnPc for 24 h. 4T1 cells without any treatment were set as control. The scale bar is 10 μm. (b) Representative flow diagrams of 4T1 tumor cells incubated with JPMO-Pt-ZnPc or JPMO-Pt-CTPP-ZnPc for 24 h. 4T1 cells without any treatment were set as control. (c) The medial fluorescent intensity of ZnPc. Each experiment was repeated three times.

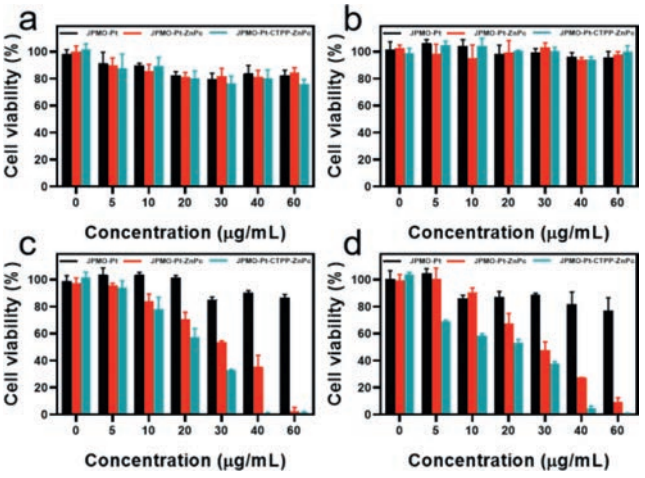

Fig. 4. (a) Viability of 4T1 cells incubated with different concentrations of JPMO-Pt, JPMO-Pt-ZnPc, and JPMO-Pt-CTPP-ZnPc in the dark for 24 h. (b) Viability of 4T1 cells incubated with different concentrations of JPMO-Pt, JPMO-Pt-ZnPc, and JPMO-Pt-CTPP-ZnPc in the dark for 48 h. (c) Viability of 4T1 cells incubated with different concentrations of JPMO-Pt, JPMO-Pt-ZnPc, and JPMO-Pt-CTPP-ZnPc after irradiation with a 660 nm laser (10 mW/cm^2) for 15 min. (d) Viability of 4T1 cells incubated with different concentrations of JPMO-Pt, JPMO-Pt-ZnPc, and JPMO-Pt-CTPP-ZnPc after irradiation with a 660 nm laser irradiation (10 mW/cm^2) for 30 min.

or 48 h, the cell viabilities all exceeded 80% (Figs. 4a and b), which indicated that the three materials all had good biocompatibility. Subsequently, we studied the PDT effects of JPMO-Pt-ZnPc and JPMO-Pt-CTPP-ZnPc on 4T1 cells. First, we assessed the cytotoxic effect of the JPMO-Pt upon irradiation with a laser at 660 nm (10 mW/cm^2). As shown in Figs. 4c and d, after 15 or 30 min of laser irradiation, the 4T1 cells incubated with different concentrations of JPMO-Pt for 24 h all showed viabilities exceeding 80%, indicating that the JPMO-Pt was not phototoxic to 4T1 cells. The results also suggested that JPMO-Pt had good biocompatibility. After 15 min of laser irradiation at 660 nm (10 mW/cm^2), 4T1 cells incubated with the JPMO-Pt-ZnPc or JPMO-Pt-CTPP-ZnPc evidently decreased in viability. Notably, at the same concentration, the viability of 4T1 cells incubated with JPMO-Pt-CTPP-ZnPc was lower than that of 4T1 cells incubated with JPMO-Pt-ZnPc (Fig. 4c). This difference is because JPMO-Pt-CTPP-ZnPc killed tumor cells more effectively by increasing the level of ROS in the mitochondria of cells due to its mitochondria-targeting effect. When the irradiation duration was extended to 30 min, the viability of the 4T1 cells incubated with low concentrations of JPMO-Pt-CTPP-ZnPc further decreased (Fig. 4d). After 30 min of laser irradiation, the viability of the 4T1 cells incubated with 60 μg/mL JPMO-Pt-CTPP-ZnPc for 24 h was only approximately 3%, indicating that the JPMO-Pt-CTPP-ZnPc exerted an excellent PDT effect on 4T1 tumor cells. Then the accumulation of the JPMO-Pt-CTPP-ZnPc in tumors was assessed in a mouse breast cancer model by intravenously injecting JPMO-Pt-CTPP-ZnPc, and the tumors of the mice showed obvious fluorescence at 24 h postinjection (Fig. S4 in Supporting information), suggesting that JPMO-Pt-CTPP-ZnPc can accumulate in tumor for further therapy.

In summary, we constructed a ZnPc-loaded CTPP-modified Janus mesoporous nanoplatform, JPMO-Pt-CTPP-ZnPc, to enhance the PDT effect. This nanoplatform had a uniform size (275 nm) and good dispersity and biocompatibility. The result of confocal laser scanning microscopy (CLSM) and flow cytometry revealed the modification of CTPP significantly improves the targeting ability of nanoplatform. *In vitro* antitumor experiments revealed the JPMO-Pt-CTPP-ZnPc significantly inhibited the growth of tumor cells upon low-power laser irradiation and that the viability of cells incubated with 60 μg/mL JPMO-Pt-CTPP-ZnPc was only 3%. The PDT effect of JPMO-Pt-CTPP-ZnPc was evidently superior to that of JPMO-Pt-ZnPc (not modified with a mitochondria-targeting molecule), indicating that the JPMO-Pt-CTPP-ZnPc produces a better PDT effect by targeting the mitochondria in cells. The PDT nanoplatform designed in this study targets the mitochondria of tumor cells and subsequently increases the killing efficacy for cancer cells, showing great potential in PDT of tumors and providing a new direction for effective tumor treatment.

Declaration of competing interest

The authors declare that they have no known competing financial interests or personal relationships that could have appeared to influence the work reported in this paper.

Acknowledgments

We greatly appreciate financial support from the National Natural Science Foundation of China (Nos. 81971675, 22275099), Project of State Key Laboratory of Organic Electronics and Information Displays, Nanjing University of Posts & Telecommunications (No. GDX2022010014), and Natural Science Research Start up Foundation of Recruiting Talents of Nanjing University of Posts and Telecommunications (No. NY222067).

Supplementary materials

Supplementary material associated with this article can be found, in the online version, at doi:10.1016/j.cclet.2023.108539.

References

[1] Y. Zhang, Y. Wan, Y. Chen, et al., ACS Nano 14 (2020) 5560–5569.
[2] Y. Yang, J. Tang, M. Zhang, et al., Nano Lett. 19 (2019) 7750–7759.
[3] P.L. Abbaraju, Y. Yang, M. Yu, et al., Chem. Asian J. 12 (2017) 1465–1469.
[4] W. Tian, S. Wang, Y. Tian, et al., J. Colloid Interface Sci. 610 (2022) 634–642.
[5] M.R. Younis, C. Wang, R. An, et al., ACS Nano 13 (2019) 2544–2557.
[6] H. Xiang, Y. Chen, Small 15 (2019) 1805339.
[7] H. Xiang, H. Lin, L. Yu, Y. Chen, ACS Nano 13 (2019) 2223–2235.
[8] L. Zhao, R. Zheng, J.Q. Huang, et al., ACS Nano 14 (2020) 17100–17113.
[9] U. Bazylinska, D. Wawrzynczyk, J. Kulbacka, et al., ACS Nano 16 (2022) 5427–5438.
[10] L. Zhao, R. Zheng, R. Kong, et al., ACS Nano 16 (2022) 1182–1197.
[11] L. Yang, P. Gao, Y. Huang, et al., Chin. Chem. Lett. 30 (2019) 1293–1296.
[12] C. Wu, Y. Li, Z. Cheng, et al., Chin. Chem. Lett. 33 (2022) 4339–4344.
[13] R. Wu, H. Wang, L. Hai, et al., Chin. Chem. Lett. 31 (2020) 189–192.
[14] D.W. Felsher, Nat. Rev. Cancer 3 (2003) 375–380.

[15] S.B. Brown, E.A. Brown, I. Walker, Lancet Oncol. 5 (2004) 497–508.
[16] D. van Straten, V. Mashayekhi, H.S. de Bruijn, S. Oliveira, D.J. Robinson, Cancers 9 (2017) 19–72.
[17] J. Guo, J. Dai, X. Peng, et al., ACS Nano 15 (2021) 20042–20055.
[18] N. Lu, W. Fan, X. Yi, et al., ACS Nano 12 (2018) 1580–1591.
[19] G. Yuan, C. Lv, J. Liang, et al., Adv. Funct. Mater. 31 (2021) 2104026.
[20] L. He, Q. Ni, J. Mu, et al., J. Am. Chem. Soc. 142 (2020) 6822–6832.
[21] Y. Tian, Y. Zhao, W. Liu, et al., RSC Adv. 8 (2018) 32200–32210.
[22] X. Wang, Y. Tian, X. Liao, et al., J. Colloid Interface Sci. 565 (2020) 483–493.
[23] C. Qi, J. He, L. Fu, et al., ACS Nano 15 (2020) 1627–1639.
[24] D. Jiang, Z.T. Rosenkrans, D. Ni, et al., Acc. Chem. Res. 53 (2020) 1869–1880.
[25] Z. Meng, Y. Zhang, E. Shen, et al., Adv. Sci. 8 (2021) 2004670.
[26] M. Lan, S. Zhao, W. Liu, et al., Adv. Healthc. Mater. 8 (2019) 1900132.
[27] Y. Yang, M. Zhang, H. Song, C. Yu, Acc. Chem. Res. 53 (2020) 1545–1556.
[28] S. Fulda, L. Galluzzi, G. Kroemer, Nat. Rev. Drug Discov. 9 (2010) 447–464.
[29] D.C. Wallace, Nat. Rev. Cancer 12 (2012) 685–698.
[30] M.P. Murphy, R.C. Hartley, Nat. Rev. Drug Discov. 17 (2018) 865–886.
[31] S.E. Weinberg, N.S. Chandel, Nat. Chem. Biol. 11 (2015) 9–15.
[32] Z. Zhou, J. Liu, T.W. Rees, et al., Proc. Natl. Acad. Sci. U. S. A. 115 (2018) 5664–5669.
[33] K. Ni, G. Lan, S. Veroneau, et al., Nat. Commun. 9 (2018) 4321.
[34] H. Zhu, B. Zhang, N. Zhu, M. Li, Q. Yu, Chin. Chem. Lett. 32 (2021) 1220–1223.
[35] S. Wang, P. Huang, X. Chen, ACS Nano 10 (2016) 2991–2994.
[36] X. Wang, L. Chen, Z. Teng, Z. Wang, Chem. Mater. 31 (2019) 3823–3830.
[37] L. Zhao, Y. Zhang, Y. Yang, C. Yu, Chem. Asian J. 17 (2022) 202200573.
[38] Z. Wu, L. Li, T. Liao, et al., Nano Today 22 (2018) 62–82.
[39] X. Du, C. Zhao, Y. Luan, et al., J. Mater. Chem. A 5 (2017) 21560–21569.
[40] H. Tang, L. Yao, J. Yang, et al., Part. Part. Syst. Charact. 33 (2016) 316–322.